Carbohydrate Polymers 117 (2015) 957–963

Contents lists available at ScienceDirect

Carbohydrate Polymers

journal homepage: www.elsevier.com/locate/carbpol

Creep behavior of starch-based nanocomposite films with cellulose nanofibrils

Meng Li [a], Dong Li [a,*], Li-jun Wang [b,*], Benu Adhikari [c]

[a] College of Engineering, National Energy R & D Center for Non-food Biomass, China Agricultural University, P. O. Box 50, 17 Qinghua Donglu, Beijing 100083, China

[b] College of Food Science and Nutritional Engineering, Beijing Key Laboratory of Functional Food from Plant Resources, China Agricultural University, Beijing, China

[c] School of Applied Sciences, RMIT University, City Campus, Melbourne, VIC 3001, Australia

ARTICLE INFO

Article history:
Received 12 June 2014
Received in revised form 4 October 2014
Accepted 6 October 2014
Available online 22 October 2014

Keywords:
Cellulose nanofibrils
Composite films
Frequency sweep
Creep behavior
Time-temperature superposition (TTS)

ABSTRACT

Nanocomposite films were successfully prepared by incorporating cellulose nanofibrils (CNFs) from sugar beet pulp into plasticized starch (PS) at CNFs concentration of 5–20%. The storage (G') and loss (G'') moduli, creep and creep-recovery behavior of these films were studied. The creep behavior of these films at long time frame was studied using time-temperature superposition (TTS). The CNFs were uniformly distributed within these films up to 15% of CNFs. The PS-only and the PS/CNFs nanocomposite films exhibited dominant elastic behavior. The incorporation of CNFs increased both the G' and G''. The CNFs improved the creep resistance and reduced the creep recovery rate of the PS/CNFs nanocomposite films. TTS method was successfully used to predict the creep behavior of these films at longer time frame. Power law and Burgers model were capable ($R^2 > 0.98$) of fitting experimental G' versus angular frequency and creep strain versus time data, respectively.

© 2014 Elsevier Ltd. All rights reserved.

1. Introduction

Growing ecological concerns and energy demands have made it imperative to develop bio-based and environment-friendly packaging materials that have good mechanical properties. Natural biodegradable polymers have more advantages over the synthetic ones because they are comparatively inexpensive and derived from renewable raw materials, agro-industrial by-products and agricultural waste (Lu, Weng, & Cao, 2005).

Among the naturally occurring renewable biopolymers, starch is one of the most abundant and low cost biodegradable materials (Mohanty, Misra, & Hinrichsen, 2000). Starch based biodegradable composites have drawn considerable attentions of the scientific community over the last two decades due to their potential applications in many industries including food (Laohakunjit & Noomhorm, 2004), packaging (Avella et al., 2005) and medicine (Krogars, Heinamaki, Antikainen, Karjalainen, & Yliruusi, 2003). However, compared with conventional synthetic materials, starch-based biodegradable products exhibit many disadvantages such as poor resistance to water, brittleness and poor elasticity. All of these disadvantages can be attributed to the highly hydrophilic characteristics of starch (Curvelo, de Carvalho, & Agnelli, 2001). One of the effective methods to improve the above mentioned properties is to incorporate various fillers. If these fillers are also derived from renewable resources, the biodegradability of the starch-based biocomposites will be preserved. Materials such as potato pulp microfibrils (Dufresne & Vignon, 1998), bleached leafwood fibers (Averous & Boquillon, 2004), tunicin whiskers (Anglès & Dufresne, 2000; Anglès & Dufresne, 2001; Mathew & Dufresne, 2002) and lignin (Lepifre et al., 2004) are used to improve the physicochemical and mechanical properties of starch-based biocomposites.

In recent years, natural cellulose nanofibrils (CNFs) are increasingly used as a loading-bearing constituent in thermoset and thermoplastic polymeric matrices (Faruk, Bledzki, Fink, & Sain, 2012; Satyanarayana, Arizaga, & Wypych, 2009). CNFs possess unique characteristics, such as high aspect ratio, high tensile strength, high Young's modulus and low coefficient of thermal expansion (Azizi Samir, Alloin, & Dufresne, 2005; Nishino, Matsuda, & Hirao, 2004). Attempts have been made in the past in producing starch-based nanocomposites reinforced with CNFs (Anglès & Dufresne, 2000; Anglès & Dufresne, 2001; Brinchi, Cotana, Fortunati, & Kenny, 2013). Lu et al. (2005) reported that the cellulose nanocrystallites derived from cottonseed linter were able to increase the Young's modulus and tensile strength of starch

* Corresponding authors. Tel.: +86 10 62737351; fax: +86 10 62737351.
E-mail addresses: dongli@cau.edu.cn (D. Li), wlj@cau.edu.cn (L.-j. Wang).

http://dx.doi.org/10.1016/j.carbpol.2014.10.023
0144-8617/© 2014 Elsevier Ltd. All rights reserved.

Nomenclature

α_T	shift factor
E_a	activation energy (kJ/mol)
R	universal gas constant (J K^{-1} mol^{-1})
T_r	reference temperature (K)
T	test temperature (K)
ε	strain of suspension
ε'	creep rate (s^{-1})
σ_0	constantly applied compressive stress (MPa)
E_K	modulus of the Kelvin spring (MPa)
E_M	modulus of the Maxwell spring (MPa)
τ	retardation time (s)
t	loading time (s)
η_M	viscosity of the Maxwell dashpot (MPa s)
η_K	viscosity of the Kelvin dashpot (MPa s)
J	creep compliance ($\mu m^2/N$)
G'	storage modulus (Pa)
G''	loss modulus (Pa)
K'	power law model constant (Pa s^n)
n'	frequency exponent (dimensionless)
R^2	correlation coefficient (dimensionless)
ω	angular frequency (rad/s)

films due to strong interactions between starch and the cellulosic nanocrystallities. The CNFs obtained from wheat straw were also found to improve the glass transition temperature (T_g) of nanocomposite films compared to pure thermoplastic starch film (Alemdar & Sain, 2008).

Most of the publications on the CNFs-reinforced nanocomposites report the mechanical properties in terms of tensile strength and compressive strength. However, viscoelastic properties are also very important characteristics of polymers which indicate the time-dependent deformation of materials as a function of temperature, stress and strain (Chen & Lai, 2008; Famá, Rojas, Goyanes, & Gerschenson, 2005). In order to determine the viscoelastic properties of composites, transient and dynamic tests can be carried out by using dynamic thermomechanical analysis (DMA). Creep and creep-recovery are the typical methods used to quantify the viscoelastic behavior of composite materials (Del Nobile, Chillo, Mentana, & Baiano, 2007). The creep-recovery behavior, quite common and useful in the life cycle of the composites, is affected by the composition of polymeric substances.

Creep is a time and temperature dependent behavior; hence, quantification of this behavior is important for assessing the durability and reliability of composite materials (Aifantis, 1987; Krempl & Khan, 2003). The Kelvin and Burgers models are most commonly used to explain the creep behavior of materials under a fixed stress (Del Nobile et al., 2007). Kelvin model consists of a spring and a dashpot in parallel. This model represents the start or early stage of creep behavior and it does not incorporate the stress relaxation aspect of a viscoelastic body. The Burgers model consists of a spring, a dashpot and a Kelvin component; hence, it is able to describe the immediate elastic deformation (ε_{SM}), the delayed elastic strain (ε_{KV}) and the Newtonian flow (ε_∞) when the composite materials are subjected to a static stress. Acha, Reboredo, and Marcovich (2007) reported that the incorporation of jute fibers in polypropylene (PP)-jute composites significantly improved their creep resistance. A good agreement between experimental data and theoretical predictions (Burgers model) were obtained in the creep region.

The frequency sweep test carried out using DMA provides melting property of materials and this test is usually carried out in liquid samples. Many material experts use DMA to study the temperature, strain rate or stress rate dependence of mechanical properties; however, only few of them study the frequency sweep. For a viscoelastic test conducted by DMA, the applied frequency plays a vital role to the mechanical response of composite materials. The viscous or liquid-like behavior predominates when the materials are subjected to a low frequency range. When the frequency is high, the materials will exhibit elastic property and appear to be stiff. This variation in viscoelastic property due to the increase in frequency is similar to the variation in the viscoelastic property due to decrease in temperature (Menard, 1999). Some studies on the frequency sweep tests (from 0.01 to 200 Hz) of the poly (vinyl alcohol) (PVA)-gelatin films containing 10–40% PVA were carried out by Mendieta-Taboada, Sobral, Carvalho, and Habitante (2008). These authors found that the value of storage modulus increased with the increase in PVA content between 10% and 30%.

In this work, we aimed at producing nanocomposite films containing starch and cellulose nanofibrils (CNFs) and investigating the viscoelastic property of these films. The creep and creep-recovery were investigated using dynamic thermomechanical analyzer (DMA). The frequency dependence of the storage and loss moduli was determined by using frequency sweep tests of DMA. Power law model was used to predict the frequency dependence of storage modulus. The Burgers model was used to predict the creep recovery. The creep behavior of these films at longer time frame was predicted using time-temperature superposition (TTS).

2. Materials and methods

2.1. Materials

Sugar beet pulp (SBP) was obtained from Xinjiang province of China. Corn starch was obtained from Hebei Zhangjiakou Yujing Food Co. Ltd. (Hebei, China). Xylitol (food grade) was purchased from Tianjin Jinguigu Science & Technology Development Co. Ltd (Tianjin, China). Sodium chlorite ($NaClO_2$) was purchased from Tianjin Guangfu Fine Chemical Research Institute (Tianjin, China). Benzene, absolute ethanol, sodium hydroxide (NaOH), glycerol and other chemicals were of analytical grade and were supplied by Beijing Chemical Works (Beijing, China).

2.2. Preparation of cellulose nanofibrils

Cellulose nanofibrils (CNFs) were produced by a method which combined chemical treatment and high pressure homogenization. A detail of this method has been reported in our previous study (Li, Wang, Li, Cheng, & Adhikari, 2014). Briefly, the de-pectinated sugar beet pulp (DSBP) powder was treated with 4% (w/v) NaOH solution at 80 °C for 2 h. This treatment was followed by bleaching (using sodium chlorite and glacial acetic acid) which was carried out at 75–80 °C for 1 h. The bleaching treatment was repeated three times. The residue obtained after bleaching was filtered and washed with distilled water until its pH was neutral. The bleached fibers were subsequently passed through a high-pressure homogenizer (AH 100D, ATS Engineering Inc, Italy) 10 times (passes) at 800 bar. The cellulose nanofibrils were obtained after this high pressure homogenization step.

2.3. Preparation of plasticized starch (PS)/CNFs nanocomposite films

The PS/CNFs nanocomposite films were prepared using solution casting method as previously used by Fu, Wang, Li, Wei, and Adhikari (2011) to prepare PS films. Corn starch, plasticizers (glycerol: xylitol ratio = 1:1), CNFs and deionized water were mixed together to form starch-plasticizer-CNFs suspension with

5.0% (w/v) solid concentration. The total concentration of the plasticizers was 30% (w/w) of the total solid content. Each batch of the suspension was thoroughly mixed by stirring at 300 rpm and was heated at 100 °C for 1 h to allow complete gelatinization of starch component. The evaporation of water during this gelatinization process was minimized by covering the beakers with six layers of water resistant films. The resulting paste was degassed under vacuum to remove the trapped air.

Films were prepared by syringing 13 mL of the paste into 9 cm diameter polycarbonate petri dishes followed by drying at 45 °C for 6 h. A series of PS/CNFs films were prepared by varying the concentration of CNFs from 5% to 20% at 5% increment and designated as PS/CNFs-5, PS/CNFs-10, PS/CNFs-15 and PS/CNFs-20, respectively. These films had a thickness of 10–50 μm. Plasticized starch only films (PS films) which did not contain CNFs were prepared in the same manner and were used as control. All of these films were equilibrated at 20 °C and 43% RH for one week using controlled humidity chambers before further tests. This equilibration to a single RH value was essential to avoid the effect of relative humidity on the viscoelastic behavior of starch-based films (Müller, Laurindo, & Yamashita, 2009).

2.4. Frequency sweep tests

The frequency sweep tests were conducted in all of the films in tension mode by using a dynamic mechanical analyzer (DMA, Q800, TA Instruments, New Castle, USA). These films were cut into 30 mm × 7 mm rectangular strips. One end of the film strip was clamped to the fixed grip and the other end was clamped to the movable grip of the DMA furnace. Then, a small preload (0.02 N) was applied to keep the film gently stretched (Pandini et al., 2012) and to establish desired film length between both ends. After equilibrating the film at 35 °C for 2 min, the frequency sweep tests were performed from 0.1 to 50 Hz. The samples were subjected to 0.05% strain which is sufficiently small to ensure that the test remained within the linear viscoelastic regime. Storage (G') and loss (G'') moduli were determined as a function of frequency. All of these tests were carried out at least three times and the average values are reported.

2.5. Creep and creep-recovery measurements

A dynamic mechanical analyzer (DMA, Q800, TA Instruments, New Castle, USA) was used to determine the creep and creep-recovery of PS/CNFs composite films and the PS-only (control) films. These tests were carried out in tension mode and at different stress levels. The specification of the films, the process of clamping or loading to the furnace the applied preload were identical to those used in frequency sweep tests (Section 2.4). The force track was set at 125%. After equilibrating at 35 °C for 2 min, a stress of 8 MPa was supplied to the films for 5 min. The stress was removed after 5 min and the films were recovered. The strain and creep compliance data was recorded as a function of time.

2.6. Time-temperature superposition (TTS)

Time-temperature superposition (TTS) was used to obtain creep deformation of the PS/CNFs and PS-only films in longer time frame. The creep tests for both types of films were carried out at six temperatures (30 °C, 35 °C, 40 °C, 45 °C, 50 °C and 55 °C) and the creep curves were obtained. These tests were carried out at a static stress of 8 MPa for 5 min. All the individual creep curves obtained at different temperatures were shifted along the logarithmic time axis to superimpose to a master curve. The horizontal shift factor α_T was calculated according to the Arrhenius equation given by Eq. (1) (Yao, Wu, Chen, & Zhang, 2013).

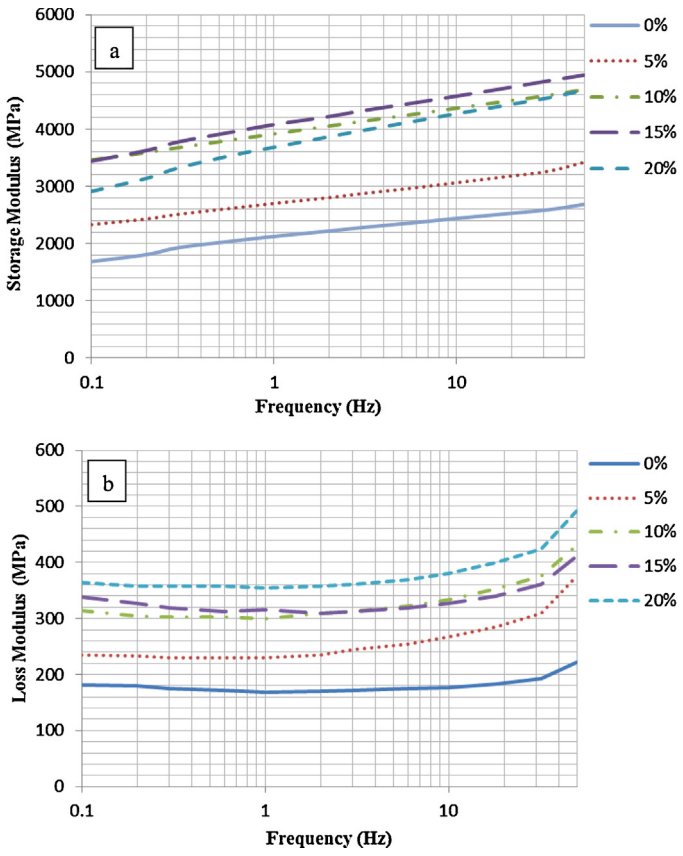

Fig. 1. The variation of (a) storage and (b) loss moduli as a function of angular frequency of starch-only and starch-cellulose nanofibrils (CNFs) composite films. The percentage values (0–20%) indicate the concentration of the CNFs in the films.

$$\log \alpha_T = \frac{E_a}{2.303R}\left(\frac{1}{T} - \frac{1}{T_r}\right) \quad (1)$$

where, E_α (kJ/mol), R (JK^{-1} mol^{-1}), T_r (K), and T(K) are the activation energy, universal gas constant, reference temperature and test temperature, respectively. Regression analysis was performed on the experimental data to fit Eq. (1). SPSS 21.0 (SPSS Inc., Chicago, USA) was used to determine the activation energy (E_α) and the associated correlation coefficient (R^2). Fifty-five (55) °C was used as the reference temperature for this purpose.

2.7. Statistical analysis

All the experiments were carried out in triplicate. The experimental DMA data was obtained directly from the Universal Analysis 2000 data analysis software (TA Instruments, New Castle, USA). Each datum is expressed as mean ± standard deviation. Duncan's multiple comparison tests were used to determine the significance difference between two mean values using SPSS 21.0 software (SPSS Inc., Chicago, USA) at 95% ($p < 0.05$) confidence level.

3. Results and discussion

3.1. The storage and loss moduli of PS/CNFs films

The storage (G') and loss (G'') moduli of starch films with and without CNFs as a function of frequency are presented in Fig. 1. Both moduli in these films increased with the increase in frequency; however, the elastic modulus (G') increased much prominently

Table 1
Power law parameters of storage modulus (G') as a function of angular frequency of starch only (PS) and starch/cellulose nanofibrils (PS/CNFs) composite films.

Samples	K' (Pa s^n)	n'	R^2
PS/CNFs-0	1881.55 ± 69.43^a	0.071 ± 0.004^a	0.981
PS/CNFs-5	2405.93 ± 7.1^b	0.059 ± 0.007^b	0.997
PS/CNFs-10	3275.1 ± 418.26^c	0.048 ± 0.005^c	0.998
PS/CNFs-15	3633.73 ± 21.73^d	0.052 ± 0.004^d	0.990
PS/CNFs-20	3170.64 ± 55.29^c	0.064 ± 0.006^e	0.982

Values represent the mean ± standard deviation of three replicates. Values in a column having different superscripts were significantly different ($p < 0.05$).
CNFs-0 to CNFs-20 represent the concentrate of the cellulose nanofibrils (CNFs) from 0% (starch-only) to 20%.

compared to the viscous modulus (G''). This is due to the fact that these composite films had longer time to relax at low frequency; hence, they appeared less elastic (less solid-like). At high frequency range, these films had less time to relax and they exhibited more elastic (solid-like) characteristics. It can also be seen from this figure that the values of storage modulus are much higher than the corresponding values of the loss modulus over the entire frequency range. These results indicate that both the starch-only and starch/CNFs composite films exhibit dominant elastic behavior than the viscous behavior (Cespi, Bonacucina, Mencarelli, Casettari, & Palmieri, 2011). The incorporation of CNFs into the starch matrix significantly ($p < 0.05$) increased both storage and loss moduli over the entire frequency range tested except in the case of 20% CNFs loading (PS/CNFs-20). These results show that the presence of CNFs in starch – CNFs composite films can enhance both the elastic and viscous behaviors of these films. This may be due to the fact that the CNFs can be homogeneously dispersed in the starch matrix and they have much higher rigidity compared to glycerol, xylitol and even the starch. Furthermore, CNFs are chemically compatible with starch and a strong hydrogen bonding occurs between CNFs and starch (Lu et al., 2005).

Power law was used to predict the frequency dependence of G' by using Eq. (2) (Tselev et al., 2004).

$$G' = K'\omega^{n'} \quad (2)$$

where, K' (**Pa s^n**) is the Power law constant which reflects the elastic property. n' (dimensionless) is the frequency exponent and ω (rad/s) is the angular frequency.

The values of K' and n' are presented in Table 1. As can be seen from this table, the regression coefficients of G' versus ω data are around 0.98–0.99 which indicate that the Power law model can fit the experimental G' versus ω data quite precisely. Furthermore, the nanocomposite films have higher K' values compared to that of the starch-only film. This indicates that the nanocomposite films are more elastic or solid-like compared to the starch-only film within the frequency range tested. All of these observations suggest that the presence of CNFs enhances the elastic component of starch-based films.

3.2. Creep and creep-recovery behavior of PS/CNFs films

Fig. 2a shows the short term creep and recovery strains of starch-only and the PS/CNFs nanocomposite films as a function of time. As can be seen from this figure, the creep and creep-recovery of the PS/CNFs composite films are quite different compared to those of starch-only films. The PS/CNFs composite films show significantly ($p < 0.05$) lower creep strain and unrecoverable strain values compared to those of the starch-only film. It is expected that the addition of CNFs into the starch matrix reduced the creep of the composite films. Thirty three percent (33%) reduction of peak creep strain was observed in PS/NCFs-5 while 69% reduction of peak creep strain was observed in PS/CNFs-15. This is due to the fact that the

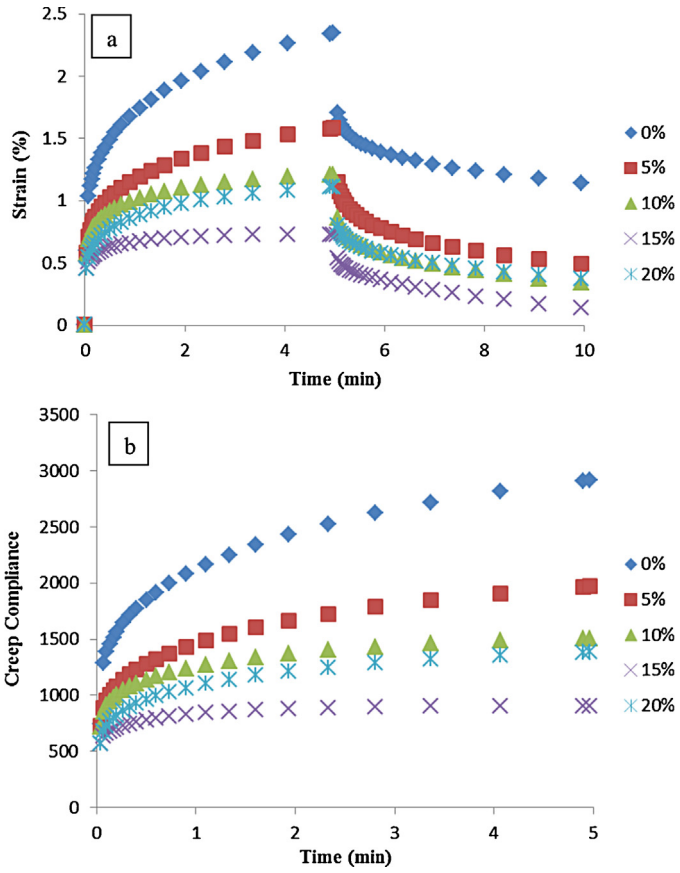

Fig. 2. The (a) creep-recovery and (b) creep compliance versus time curves of starch-only and starch-cellulose nanofibrils (CNFs) composite films. The percentage values (0–20%) indicate the concentration of the CNFs in the films.

incorporated and well dispersed NCFs greatly decrease the mobility of starch chains when external stress is applied and they can bear higher loads (Yang, Zhang, Schlarb, & Friedrich, 2006). However, the creep strain does not decrease monotonously with the increase of CNFs concentration. When the CNFs content increased to 20%, the films showed higher creep strain and higher unrecoverable strain compared to those containing lower concentration of CNFs. This is due to the fact that CNFs concentration of 20% or higher cannot be uniformly dispersed throughout the starch matrix. As a consequence, the creep behavior of the composite films could not be constrained. The incorporation of CNFs could improve creep-resistance of starch films and this reinforcing effect increases with the increase of CNFs up to 15%.

In the recovery stage, strain recovery in all samples is below 100% due to the viscous nature of these films. The greater elasticity for the starch-only matrix film is recovered. A larger deformation of the viscous component was observed in starch-only films compared to that in CNFs containing composite films. The unrecovered strain of PS/CNF-5 and PS/CNF-15 deceased 57% and 88%, respectively, compared to the control film.

Fig. 2b shows a comparative analysis of creep compliance in starch-only and PS/CNFs nanocomposite films as a function of time. This figure shows that there is a remarkable decrease in the magnitude of creep compliance in starch films due to the incorporation of CNFs. When the CNFs content was up to 15%, it can be observed that the creep compliance decreased with the increase in CNFs concentration as was observed in creep and creep-recovery data. This observation also indicates to the improvement in creep resistance in PS/CNFs films due to increased interaction between starch and CNFs. These results illustrate that the CNFs are effective in retarding

Table 2
The parameters of the Burgers models for starch only (PS/CNFs-0) and nanocomposite films (PS/CNFs-5 to PS/CNFs-20).

Samples	E_M (× 10^3 MPa)	E_K (× 10^3 MPa)	τ (s)	η_M (× 10^3MPa s)	R^2	ε' (∞) × 10^{-5} s^{-1})
PS/CNFs-0	1.135 ± 0.038[a]	1.000 ± 0.108[a]	12.939 ± 1.504[a]	293.662 ± 35.480[a]	0.981	2.750 ± 0.318[a]
PS/CNFs-5	1.277 ± 0.017[b]	1.504 ± 0.102[b]	24.281 ± 0.850[b]	526.403 ± 32.211[b]	0.992	1.523 ± 0.092[b]
PS/CNFs-10	1.382 ± 0.043[c]	2.007 ± 0.070[c]	20.386 ± 0.544[c]	1171.312 ± 364.905[c]	0.986	0.724 ± 0.197[c]
PS/CNFs-15	1.768 ± 0.044[d]	3.735 ± 0.252[d]	20.897 ± 0.367[c]	4291.295 ± 813.085[d]	0.983	0.191 ± 0.037[d]
PS/CNFs-20	1.679 ± 0.035[e]	2.087 ± 0.111[e]	23.72 ± 1.307[b]	938.059 ± 72.263[e]	0.991	0.856 ± 0.063[e]

Values represent the mean ± standard deviation of three replicates. Values in a column having different superscripts were significantly different ($p < 0.05$).
CNFs-0 to CNFs-20 represent the concentrate of the cellulose nanofibrils (CNFs) from 0% (starch-only) to 20%.

and restricting the mobility of starch chains. However, when the CNFs concentration reached 20%, both the storage and loss moduli decreased to some extent. This observation indicates that there is a limit or ceiling CNFs concentration up to which the mechanical properties of the films can be improved, in this case of PS/CNFs composite films, it appears to be 15%.

A four-parameter Burgers model (Eq. (3)), which combines Maxwell and Kelvin-Voigt elements, is widely used to represent the creep behavior of viscoelastic materials (Ward, 1983; Findley, Lai, & Onaran, 1989). In the case of a linear viscoelastic solid, the total creep strain consists of three essentially separate parts. The first part is the immediate elastic deformation (first term to the right-hand side of Eq. (3)) which is a constant value and does not change with time. The second part is the delayed elastic strain (second term in the right-hand side of Eq. (3)) which represents the earliest stage of creep and attains a saturation value in short time. The third part is the Newtonian flow (last term in the right-hand side of Eq. (3)) which represents the trend in the creep strain at sufficiently long time, and appears similar to the deformation of a viscous liquid obeying Newton's law of viscosity.

$$\varepsilon_B = \frac{\sigma_0}{E_M} + \frac{\sigma_0}{E_K}\left(1 - e^{-t/\tau}\right) + \frac{\sigma_0}{\eta_M}t \quad (3)$$

In Eq. (3), ε_B (dimensionless) represents the creep strain of a film, t denotes the time (s) after loading, σ_0 represents the loaded stress. E_M and η_M represent the modulus and viscosity of the Maxwell spring and dashpot, respectively. $\tau = \eta_K/E_k$, is the retardation time taken to produce 63.2% or $(1 - e^{-1})$ of the total deformation in the Kelvin unit. E_K and η_K represent the modulus and viscosity of the Kelvin spring and dashpot, respectively. The experimental ε_B versus t data were fitted to the Eq. (3) with SPSS 21.0 (SPSS Inc., Chicago, USA), and the four parameters (E_M, E_K, η_M, and τ) were obtained.

The values of the above mentioned four parameters for the test films are listed in Table 2. As shown in Table 2, the Burgers model shows a satisfactory agreement with the experimental strain versus time data ($R^2 > 0.981$). PS/CNFs nanocomposite films showed higher values of the viscoelastic and viscoplastic parameters than those of control film. The parameter E_K, representing the modulus of Maxwell spring causes instantaneous elastic creep strain which is immediately recovered after the removal of stress. Among the PS/CNFs nanocomposite films, the film containing 15% CNFs (PS/CNFs-15) showed the highest elasticity value while the starch (PS)-only film had the lowest elasticity. These results indicate, once again, that the incorporation of CNFs improves the elasticity of the starch-based films.

The retardant elasticity (E_K) in the Kelvin unit represents the stiffness of amorphous polymer chains in short time frame. The magnitude of E_K increased significantly ($p < 0.05$) when the CNFs were added. As pointed out in the preceding section this is due to the decreased mobility of the starch chains in the presence of CNFs. The parameter η_K presents the viscosity of the Kelvin-Voigt unit and the retardation time τ is the ratio of η_K to E_K. The retardation time increased with the incorporation of CNFs in starch films compared to that of only-starch film. The retardation time was not significantly ($p > 0.05$) different among the PS/CNFs nanocomposite

Table 3
The activation energy (E_α) values calculated using Arrhenius equation for starch only (PS/CNFs-0) and nanocomposite (PS/CNFs-5 to PS/CNFs-20) films.

Sample	E_α (KJ/mol)	R^2
PS/CNFs-0	75.736[a]	0.991
PS/CNFs-5	117.761[b]	0.977
PS/CNFs-10	130.857[c]	0.999
PS/CNFs-15	166.539[d]	0.998
PS/CNFs-20	125.662[e]	0.986

Values in a column having different superscripts were significantly different ($p < 0.05$).
CNFs-0 to CNFs-20 represent the concentrate of the cellulose nanofibrils (CNFs) from 0% (starch-only) to 20%.

films. The parameter η_M represents the irrecoverable creep strain due to the damage in the crystalline structure of polymer or the damage in the orientation of the noncrystalline region. η_M also represents the irreversible deformation of amorphous region such as breaking of bridging segments, separation of junctions between CNFs and starch chains and pulling out of chain entanglements (Yang et al., 2006). The magnitude of η_M increased much more prominently compared to that of η_K due to the addition of CNFs which indicates that the viscous flow (contribution of dashpot component in the model) and the irreversible deformation were much lower.

Based on the Burgers model, the creep rate can be calculated by differentiating Eq. (3) as shown in the following equation:

$$\varepsilon'(t) = \frac{d\varepsilon(t)}{dt} = \frac{\sigma_0}{\eta_K}e^{-t/\tau} + \frac{\sigma_0}{\eta_M} \quad (4)$$

After a sufficient long time, the creep rate will gradually attain a constant value in the steady creep stage ($t = \infty$) as shown by in Eq. (5).

$$\varepsilon'(\infty) = \left.\frac{d\varepsilon(t)}{dt}\right|_{t=\infty} = \frac{\sigma_0}{\eta_M} \quad (5)$$

The ε' (∞) is also listed in Table 2. As can be seen from this table, the final creep rate has decreased significantly ($p < 0.05$) when the CNFs are incorporated in the starch film. The extent of decease in the creep rate suggests that structure of these nanocomposite films is quite different compared to the starch-only film (due to the presence of CNFs).

3.3. Time-temperature superposition (TTS)

The creep curves of the films were determined at different temperatures and are presented in Fig. 3. The creep strain has decreased with the increase in temperature (30–55 °C) in all the samples. The creep curves were shifted according to the TTS principle, selecting 55 °C as the reference temperature (T_f), and the resulting TTS master curves are presented in Fig. 4. The temperature dependence of the shift factors showed a good linear relationship with the absolute temperature ($R^2 > 0.985$) as shown in Fig. 4. The activation energy (E_a) values of these films are summarized in Table 3. To predict the long term creep behavior from short term measurements,

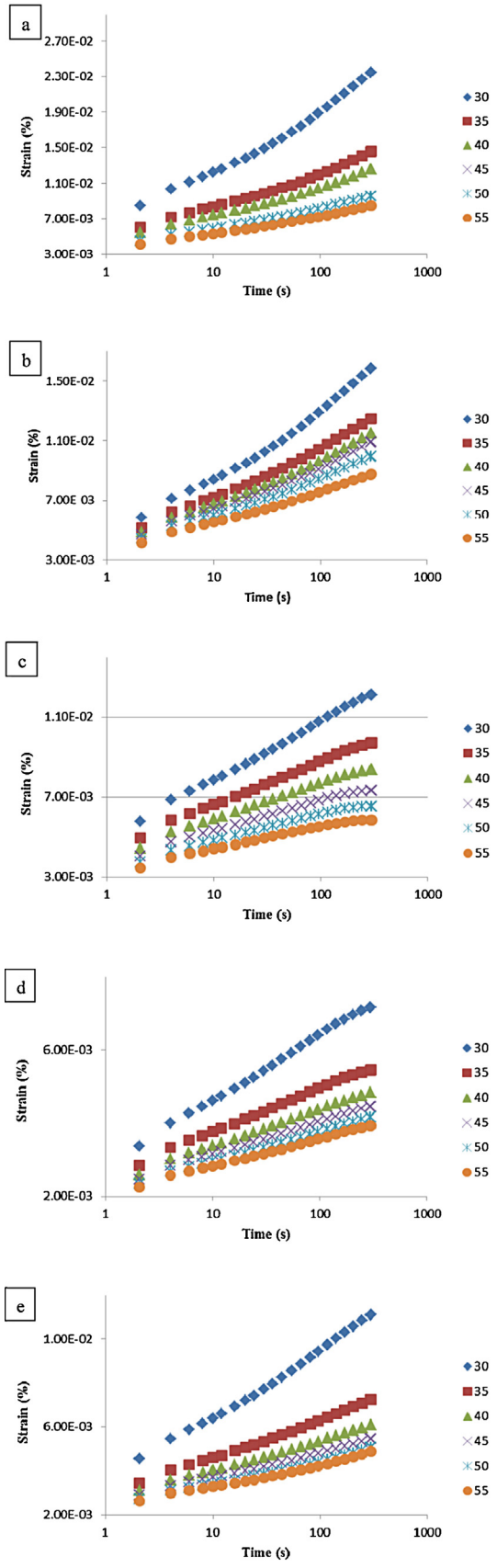

Fig. 3. The variation of creep strain of starch (PS)-only film and PS/cellulose nanofibrils (CNFs) nanocomposite films at different temperatures and at different concentration of the CNFs. (a) 0%, (b) 5%, (c) 10%, (d) 15% and (e) 20%.

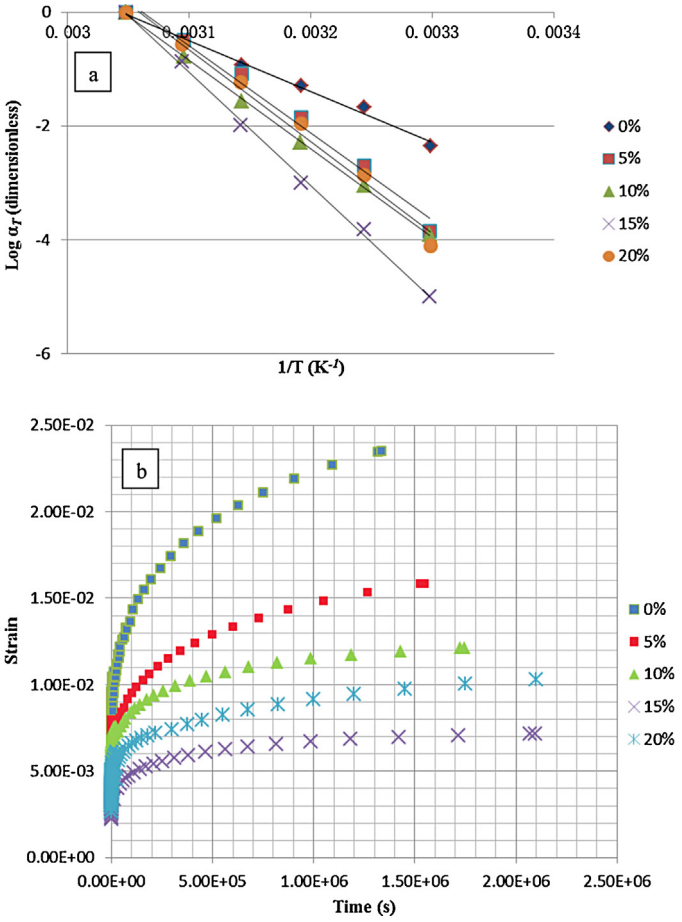

Fig. 4. The (a) shift factor and (b) TTS master curves for starch (PS)-only and PS/celluose nanofibrils (CNFs) composite films. The 0–20% indicate the concentration of CNFs.

it is often assumed that the structure of these composite films do not change with time, therefore the TTS principle holds, but this assumption cannot be taken as a valid inference without some priori validation work. The principle of TTS was recently applied to evaluate polyurethane-carbon nanotube composites and the outcome was found to be satisfactory (Yao et al., 2013). As can be seen from the TTS master curve (Fig. 4b), the creep strain (in longer time frame) of the nanocomposite films was lower than that of starch (PS)-only film which indicates to the reinforced creep resistance due to the presence of CNFs. The creep strain of the nanocomposite films (in longer time frame) decreased with the increase in CNFs except when their concentration was 20% (PS/CNFs-20). As explained in preceding section, it is difficult to uniformly disperse the CNFs at 20% concentration and they selectively concentrate or aggregate in the films. Both factors led to the reduction of creep resistance in the film.

The nanocomposite films had significantly ($p < 0.05$) higher activation energy compared to the starch (PS)-only film (Table 3). Specifically, the PS/CNFs-15 had the highest activation energy (166.539 KJ/mol) while the starch-only film had the lowest one (75.736 KJ/mol). This indicates that higher energy is required for the mobility of starch molecules in these composite films due to motion restricting effect of CNFs on the chain mobility. The higher storage modulus values in the nanocomposite films can be another reason that nanocomposite films would require more energy during creep tests.

4. Conclusions

Storage modulus, loss modulus and creep behavior of starch-only and starch –cellulose nanofibrils (CNFs) composite films were investigated. The starch only and PS/CNFs films exhibited dominant elastic behavior (than viscous behavior). The incorporation of CNFs increased both the storage (G') and loss (G'') modulus significantly ($p < 0.05$). Power law model was found to fit the experimental G' versus angular frequency data well ($R^2 > 0.981$). The presence of CNFs in PS/CNFs nanocomposite films was found to significantly decrease the creep strain, creep compliance and creep rate at longer time frame. The concentration of CNFs at and above 20% found to decrease G' and increase the creep behavior due to poor dispersion. Nanocomposite films with 15% CNFs showed the lowest creep level and the highest G'. The creep behavior of all the films was found to be predicted by the Burgers model well ($R^2 > 0.981$). The parameters of the Burgers model were significantly ($p < 0.05$) affected by the presence of the CNFs. The time–temperature superposition (TTS) method was successfully used to predict the creep behavior of PS/CNFs films at longer time frame.

Acknowledgments

This research was supported by High Technology Research and Development Program of China (2011AA100802), Science and Technology Support Project of China (2013BAD10B03) and Commonwealth Guild Agricultural Scientific Research Program of China (201003077).

References

Acha, B. A., Reboredo, M. M., & Marcovich, N. E. (2007). Creep and dynamic mechanical behavior of PP-jute composites: Effect of the interfacial adhesion. *Composites Part A: Applied Science and Manufacturing*, *38*(6), 1507–1516.

Aifantis, E. C. (1987). The physics of plastic deformation. *International Journal of Plasticity*, *3*(3), 211–247.

Alemdar, A., & Sain, M. (2008). Biocomposites from wheat straw nanofibers: Morphology, thermal and mechanical properties. *Composites Science and Technology*, *68*(2), 557–565.

Anglès, M. N., & Dufresne, A. (2000). Plasticized starch/tunicin whiskers nanocomposites. 1. Structural analysis. *Macromolecules*, *33*(22), 8344–8353.

Anglès, M. N., & Dufresne, A. (2001). Plasticized starch/tunicin whiskers nanocomposite materials. 2. Mechanical behavior. *Macromolecules*, *34*(9), 2921–2931.

Avella, M., De Vlieger, J. J., Errico, M. E., Fischer, S., Vacca, P., & Volpe, M. G. (2005). Biodegradable starch/clay nanocomposite films for food packaging applications. *Food Chemistry*, *93*(3), 467–474.

Averous, L., & Boquillon, N. (2004). Biocomposites based on plasticized starch: Thermal and mechanical behaviours. *Carbohydrate Polymers*, *56*(2), 111–122.

Azizi Samir, M. A. S., Alloin, F., & Dufresne, A. (2005). Review of recent research into cellulosic whiskers, their properties and their application in nanocomposite field. *Biomacromolecules*, *6*(2), 612–626.

Brinchi, L., Cotana, F., Fortunati, E., & Kenny, J. M. (2013). Production of nanocrystalline cellulose from lignocellulosic biomass: Technology and applications. *Carbohydrate Polymers*, *94*(1), 154–169.

Cespi, M., Bonacucina, G., Mencarelli, G., Casettari, L., & Palmieri, G. F. (2011). Dynamic mechanical thermal analysis of hypromellose 2910 free films. *European Journal of Pharmaceutics and Biopharmaceutics*, *79*(2), 458–463.

Chen, C., & Lai, L. (2008). Mechanical and water vapor barrier properties of tapioca starch/decolorized hsian-tsao leaf gum films in the presence of plasticizer. *Food Hydrocolloids*, *22*(8), 1584–1595.

Curvelo, A. A. S., de Carvalho, A. J. F., & Agnelli, J. A. M. (2001). Thermoplastic starch–cellulosic fibers composites: Preliminary results. *Carbohydrate Polymers*, *45*(2), 183–188.

Del Nobile, M. A., Chillo, S., Mentana, A., & Baiano, A. (2007). Use of the generalized Maxwell model for describing the stress relaxation behavior of solid-like foods. *Journal of Food Engineering*, *78*(3), 978–983.

Dufresne, A., & Vignon, M. R. (1998). Improvement of starch film performances using cellulose microfibrils. *Macromolecules*, *31*(8), 2693–2696.

Famá, L., Rojas, A. M., Goyanes, S., & Gerschenson, L. (2005). Mechanical properties of tapioca-starch edible films containing sorbates. *LWT—Food Science and Technology*, *38*(6), 631–639.

Faruk, O., Bledzki, A. K., Fink, H., & Sain, M. (2012). Biocomposites reinforced with natural fibers: 2000–2010. *Progress in Polymer Science*, *37*(11), 1552–1596.

Findley, W. N., Lai, J. S., & Onaran, K. (1989). *Creep and relaxation of nonlinear viscoelastic materials: With an introduction to linear viscoelasticity*. New York: Dover Publication, Inc.

Fu, Z., Wang, L., Li, D., Wei, Q., & Adhikari, B. (2011). Effects of high-pressure homogenization on the properties of starch-plasticizer dispersions and their films. *Carbohydrate Polymers*, *86*(1), 202–207.

Krempl, E., & Khan, F. (2003). Rate (time)-dependent deformation behavior: An overview of some properties of metals and solid polymers. *International Journal Of Plasticity*, *19*(7), 1069–1095.

Krogars, K., Heinamaki, J., Antikainen, O., Karjalainen, M., & Yliruusi, J. (2003). A novel amylose corn-starch dispersion as an aqueous film coating for tablets. *Pharmaceutical Development and Technology*, *8*(3), 211–217.

Laohakunjit, N., & Noomhorm, A. (2004). Effect of plasticizers on mechanical and barrier properties of rice starch film. *Starch—Stärke*, *56*(8), 348–356.

Lepifre, S., Froment, M., Cazaux, F., Houot, S., Lourdin, D., Coqueret, X., et al. (2004). Lignin incorporation combined with electron-beam irradiation improves the surface water resistance of starch films. *Biomacromolecules*, *5*(5), 1678–1686.

Li, M., Wang, L., Li, D., Cheng, Y., & Adhikari, B. (2014). Preparation and characterization of cellulose nanofibers from de-pectinated sugar beet pulp. *Carbohydrate Polymers*, *102*, 136–143.

Lu, Y., Weng, L., & Cao, X. (2005). Biocomposites of plasticized starch reinforced with cellulose crystallites from cottonseed linter. *Macromolecular Bioscience*, *5*(11), 1101–1107.

Mathew, A. P., & Dufresne, A. (2002). Morphological investigation of nanocomposites from sorbitol plasticized starch and tunicin whiskers. *Biomacromolecules*, *3*(3), 609–617.

Menard, K. P. (1999). Chapter 7: Frequency scans. In P. Kevin Menard (Ed.), *Dynamic mechanical analysis: A practical introduction* (pp. 160–180). Boca Raton, Florida, USA: CRC Press.

Mendieta-Taboada, O., Sobral, P. J. D. A., Carvalho, R. A., & Habitante, A. M. B. Q. (2008). Thermomechanical properties of biodegradable films based on blends of gelatin and poly(vinyl alcohol). *Food Hydrocolloids*, *22*(8), 1485–1492.

Müller, C. M. O., Laurindo, J. O. B., & Yamashita, F. (2009). Effect of cellulose fibers on the crystallinity and mechanical properties of starch-based films at different relative humidity values. *Carbohydrate Polymers*, *77*(2), 293–299.

Mohanty, A. K., Misra, M., & Hinrichsen, G. (2000). Biofibres, biodegradable polymers and biocomposites: An overview. *Macromolecular Materials and Engineering*, *276–277*(1), 1–24.

Nishino, T., Matsuda, I., & Hirao, K. (2004). All-cellulose composite. *Macromolecules*, *37*(20), 7683–7687.

Pandini, S., Passera, S., Messori, M., Paderni, K., Toselli, M., Gianoncelli, A., et al. (2012). Two-way reversible shape memory behaviour of crosslinked poly(ε-caprolactone). *Polymer*, *53*(9), 1915–1924.

Satyanarayana, K. G., Arizaga, G. G. C., & Wypych, F. (2009). Biodegradable composites based on lignocellulosic fibers—an overview. *Progress in Polymer Science*, *34*(9), 982–1021.

Tselev, A., Brooks, C. M., Anlage, S. M., Zheng, H., Salamanca-Riba, L., Ramesh, R., et al. (2004). Evidence for power-law frequency dependence of intrinsic dielectric response in the CaCu3Ti4O12. *Physical Review B*, *70*(14410114).

Yang, J., Zhang, Z., Schlarb, A. K., & Friedrich, K. (2006). On the characterization of tensile creep resistance of polyamide 66 nanocomposites. Part I. Experimental results and general discussions. *Polymer*, *47*(8), 2791–2801.

Yao, Z., Wu, D., Chen, C., & Zhang, M. (2013). Creep behavior of polyurethane nanocomposites with carbon nanotubes. *Composites Part A: Applied Science and Manufacturing*, *50*, 65–67.